Published in final edited form as:
Cell Calcium. 2009 April ; 45(4): 400–411. doi:10.1016/j.ceca.2009.01.004.

Opposite regulation of KCNQ5 and TRPC6 channels contributes to vasopressin-stimulated calcium spiking responses in A7r5 vascular smooth muscle cells

Bharath K. Mani[1], **Lioubov I. Brueggemann**[1], **Leanne L. Cribbs**[2], and **Kenneth L. Byron**[1]

[1] Department of Pharmacology and Experimental Therapeutics, Loyola University Chicago, Maywood, IL- 60153

[2] Department of Medicine/Cardiovascular Institute, Loyola University Chicago, Maywood, IL - 60153

Summary

Physiologically relevant concentrations of [Arg^8]-vasopressin (AVP) induce repetitive action potential firing and Ca^{2+} spiking responses in the A7r5 rat aortic smooth muscle cell line. These responses may be triggered by suppression of KCNQ potassium currents and/or activation of non-selective cation currents. Here we examine the relative contributions of KCNQ5 channels and TRPC6 non-selective cation channels to AVP-stimulated Ca^{2+} spiking using patch clamp electrophysiology and fura-2 fluorescence measurements in A7r5 cells. KCNQ5 or TRPC6 channel expression levels were suppressed by short hairpin RNA constructs. KCNQ5 knockdown resulted in more positive resting membrane potentials and induced spontaneous action potential firing and Ca^{2+} spiking. However physiological concentrations of AVP induced additional depolarization and increased Ca^{2+} spike frequency in KCNQ5 knockdown cells. AVP-activated non-selective cation current was reduced by TRPC6 shRNA treatment or removal of external Na^+. Neither resting membrane potential nor the AVP-induced depolarization was altered by knockdown of TRPC6 channel expression. However, both TRPC6 shRNA and removal of external Na^+ delayed the onset of Ca^{2+} spiking induced by 25 pM AVP. These results suggest that suppression of KCNQ5 currents alone is sufficient to excite A7r5 cells, but AVP-induced activation of TRPC6 contributes to the stimulation of Ca^{2+} spiking.

Keywords

Vasopressin; calcium spiking; KCNQ; TRPC6; resting membrane potential

1. Introduction

[Arg^8]-vasopressin (AVP) is a pituitary hormone that is released into the systemic circulation when blood pressure falls. Circulating concentrations of AVP may increase from a few picomolar to several hundred picomolar in response to a large drop in blood pressure [1]. AVP binding to V_{1a} vasopressin receptors on vascular smooth muscle cells (VSMCs) is known to

Corresponding Author: Dr. Kenneth L. Byron, Loyola University Medical Center, 2160 S. First Avenue, Maywood, IL 60153, Tel.: 708-327-2819, Fax: 708-216-6596, kbyron@lumc.edu.

induce Ca^{2+} release from the sarcoplasmic reticulum and Ca^{2+} influx via multiple Ca^{2+}-permeable non-selective cation channels [2,3]. The resulting elevation of cytosolic Ca^{2+} concentration ($[Ca^{2+}]_i$) activates the contractile apparatus of the vascular smooth muscle cells in the artery walls and leads to vasoconstriction. This mechanism is generally thought to be essential for the well characterized ability of AVP to restore blood pressure.

More recently, it has become apparent that AVP can induce Ca^{2+} responses in vascular smooth muscle cells via two distinct concentration-dependent pathways [4–6]. At physiological (picomolar) concentrations of AVP, inhibition of KCNQ family potassium currents results in membrane depolarization and activation of voltage-sensitive Ca^{2+} channels; the resulting influx of Ca^{2+} increases $[Ca^{2+}]_i$ [4–6]. Nanomolar concentrations of AVP induce a robust Ca^{2+} release from the sarcoplasmic reticulum mediated through the classical receptor-activated phospholipase (PLC)/inositol triphosphate (IP_3)-diacylglycerol (DAG) pathway [2,3]. Although the clinical use of AVP [7] and V_{1a} vasopressin receptor antagonists [8,9] for a plethora of indications has increased significantly in recent years, the mechanisms of action of physiologically or therapeutically relevant concentrations of AVP still remain to be clarified.

The recently proposed hypothesis that KCNQ (Kv7) family of K^+ channels might be the downstream target of physiological concentrations of AVP [4] has yet to be fully accepted. KCNQ channels were first discovered in neurons and recognized as the molecular correlate of M-currents [10]. Five members have been recognized in the KCNQ channel family (Kv7.1–7.5) [11,12]. Though expression was initially thought to be restricted to neurons and cardiac myocytes, KCNQ channels have now been shown to be expressed in many cell types, including VSMCs [4,6,12–14]. KCNQ channels conduct voltage-dependent non-inactivating outward K^+ currents that tend to oppose membrane depolarization to the threshold for triggering action potential generation; hence they act as a brake for neuronal excitation [15]. These properties of KCNQ channels may also enable them to serve as regulators of excitation of VSMCs. We previously provided evidence that physiological concentrations (10–100 pM) of AVP indeed produce membrane depolarization and Ca^{2+} influx in A7r5 rat aortic smooth muscle cells through a protein kinase C (PKC)-dependent suppression of KCNQ5 currents [4]. We also showed that KCNQ currents in freshly isolated rat mesenteric artery smooth muscle cells are similarly regulated by AVP [6].

However, KCNQ channel inhibition may not be the only mechanism by which AVP regulates membrane excitability to increase $[Ca^{2+}]_i$ in VSMCs. Signal transduction mediators implicated in KCNQ current suppression have also been implicated as regulators of other membrane-depolarizing effectors. For example, DAG, not only activates PKC and consequently suppresses KCNQ currents, but also activates non-selective cation channels independently of PKC activation [16]. The DAG-sensitive TRPC6 channel has been proposed as a candidate cation channel that could increase $[Ca^{2+}]_i$ following stimulation of G protein coupled receptors [17,18]. TRPC6 is a member of the transient receptor potential (TRP) superfamily of cation-selective ion channels. An earlier attempt to implicate TRPC6 in AVP signaling used a supraphysiological concentration of AVP (100 nM) [18] at which AVP increases $[Ca^{2+}]_i$ by stimulating both Ca^{2+} release and Ca^{2+} influx. In the present study, we have examined the contribution of TRPC6 at physiological concentrations of AVP (10–100 pM) that stimulate action potential-mediated Ca^{2+} spiking, a phenomenon that is independent of the release of intracellular Ca^{2+} stores [19]. Our findings demonstrate that KCNQ5 channels are essential channels that conduct K^+ at resting membrane potential and implicate both TRPC6 channel activation and KCNQ5 channel suppression in the stimulation of Ca^{2+} spiking by physiological concentrations of AVP in A7r5 cells.

2. EXPERIMENTAL PROCEDURES

2.1 Construction of adenovirus to express TRPC6-shRNA or KCNQ5-shRNA

For RNA interference, short hairpin RNAs (shRNAs) were designed against the rat TRPC6 sequence, 5′-GAAGGTCTTTATGCAATCGCGGTGGTTTT-3′ and the KCNQ5 sequence 5′-GGCTTCAAGTTGCCTCTTAATTCTGGAGT-3′. A control nucleotide sequence shRNA was made against the scrambled nonsense sequence 5′-TGCAGCTGTGGTCGCCCAGATTCGCCGAC-3′. Complementary nucleotides encoding the short hairpin sequences were cloned into RNAi-Ready pSIREN-DNR-DsRed-Express shuttle vector, and the recombinant shuttle vector was then used to construct the “AdenoX-TRPC6sh” or “AdenoX-KCNQ5sh” adenovirus using the Knockdown Adenoviral RNAi System 2 (BD Clontech). The AdenoX-TRPC6sh or KCNQ5sh adenovirus plasmid was digested with Pac I prior to transfection into HEK-293 cells using SuperFect Transfection Reagent (Qiagen). Within 7–10 days, when red-fluorescent plaques and cytopathic effects were apparent, lysates were prepared and used for adenovirus amplification and purification. Purified adenovirus was used directly on A7r5 cells in culture at a multiplicity of infection (MOI) of 50. Infected cells could be identified by red fluorescence within 24 hours.

2.2 A7r5 cell culture

A7r5 cells derived from embryonic rat aorta were cultured as described previously [19]. Cells were sub-cultured in 6-well plates for fura-2 fluorescence measurements. Appropriate experimental groups were infected for 3–5 days with an adenoviral vector to co-express the fluorescent marker DsRed with TRPC6, KCNQ5, or scrambled control shRNAs.

2.3 $[Ca^{2+}]_i$ measurements with fura-2

Confluent monolayers of A7r5 cells cultured in 6-well plates were washed twice with control medium (135 mM NaCl, 5.9 mM KCl, 1.5 mM $CaCl_2$, 1.2 mM $MgCl_2$, 11.5 mM glucose, 11.6 mM HEPES, pH 7.3) and then incubated in the same medium with 1 μM fura-2-AM (Invitrogen/Molecular Probes), 0.1% bovine serum albumin and 0.02% Pluronic F127 detergent for 60 min at room temperature (22–25°C) in the dark. The cells were then washed twice and incubated in the dark in control medium for 1.5 h. Sodium-free medium contained 135mM N-methyl D-glucamine (NMDG) instead of sodium. Fura-2 fluorescence was measured using a Biotek Synergy™ HT plate reader (340 and 380 nm excitation; 510 nm emission). All experiments were performed at room temperature. Prior to loading the cells with fura-2-AM, cells were observed with a fluorescence microscope for DsRed fluorescence (535 nm excitation wavelength, 610 nm emission wavelength) to confirm the expression of TRPC6 or KCNQ5 shRNA. Background fluorescence at 340 and 380 nm wavelengths was also measured in the Biotek plate reader in the same wells before the start of fura-2 loading and subtracted from individual wavelength measurements before calculating 340/380 fluorescence ratio. The latency to onset of spiking was measured as the time from the start of treatment to the start of repetitive Ca^{2+} spiking (at least 2 spikes/min). Frequency of spiking was calculated by the number of spikes per min from the time of onset of repetitive Ca^{2+} spiking. Each ‘n’ is an average value of 3 wells tested. The frequency of spiking and the latency to start of repetitive Ca^{2+} spiking were compared among control and treatment groups using Student’s paired ‘t’ test or one way analysis of variance (ANOVA) as appropriate, with ‘p’ values < 0.05 considered statistically significant.

2.4 Electrophysiology

The whole cell perforated patch configuration was used to measure KCNQ5 currents under voltage-clamp conditions and membrane potentials under current-clamp conditions in single A7r5 cells trypsinized and plated on glass coverslips; the ruptured patch configuration was

used to measure TRPC6 currents. All experiments were performed at room temperature with continuous perfusion of bath solution. The standard bath solution contained (in mM): 5 KCl, 135 NaCl, 10 HEPES, 2 $CaCl_2$, 1.2 $MgCl_2$, 5 glucose, pH 7.3. To isolate KCNQ currents, 100 μM $GdCl_3$ (sufficient to block L- and T-type Ca^{2+} channels and non-selective cation channels) was added to the standard external solution. Internal (pipette) solution to record KCNQ currents contained (in mM): 110 K gluconate, 30 KCl, 5 HEPES, 1 K_2EGTA, 1 $MgCl_2$, pH 7.2. Osmolality was adjusted to 270 mOsm/l with D-glucose. 200 μg/ml Amphotericin B was added to the internal solution for membrane patch perforation. KCNQ currents were recorded in perforated patch configuration by application of 5 s voltage steps from a −74 mV holding potential to test potentials ranging from −94 mV to +46 mV. The series resistance in perforated patch recordings was below 30 MΩ. I_{CAT} activated by 100 nM AVP was recorded in ruptured patch configuration with a 100 ms voltage ramp protocol (from +85 to −115 mV) from −15 mV holding potential every 5 sec. Internal solution to record I_{CAT} contained (in mM): 110 Cs aspartate, 30 CsCl, 5 HEPES, 1 Cs_2EGTA, 1 $MgCl_2$, 2 Na_2ATP, pH 7.2. Osmolality was adjusted to 270 mOsm/l with D-glucose. 10 μM verapamil and 100 μM spermine chloride were added to the external solution to block L-type Ca^{2+} channels and Mg^{2+}-inhibitable currents, respectively. Sodium-free medium contained 135 mM NMDG instead of Na^+. In knockdown experiments, current densities or membrane potentials were measured in control A7r5 cells and in brightly DsRed fluorescent cells. Current-clamp recording of membrane potential was performed in $I = 0$ mode. Data are presented as mean ± standard error of the mean (S.E.). For comparisons between groups, rank sum test, student's paired 't' test or one-way analysis of variance (ANOVA) was used, with 'p' values < 0.05 considered statistically significant.

2.5 Immunohistochemical detection of TRPC6 and KCNQ5

A7r5 cells were infected with adenoviral vectors for TRPC6shRNA or KCNQ5shRNA for 5 days. The cells were then trypsinized, resuspended with an equal number of uninfected control A7r5 cells, and then re-plated on 12 mm round glass coverslips 1 day prior to fixing. The cells were fixed with 2% paraformaldehyde in phosphate-buffered saline. Coverslips with KCNQ5shRNA-expressing cells were incubated with rabbit polyclonal anti-KCNQ5 antibodies (Chemicon Inc) at a 1:2000 dilution at 4°C overnight. Coverslips with TRPC6shRNA-expressing cells were incubated with rabbit polyclonal anti-TRPC6 antibodies (Alomone Labs) at a 1:200 dilution at 4°C over night. Alexa Fluor® 488 goat anti-rabbit IgG at 1:400 dilution was used as secondary antibody. Cell images were acquired with an Olympus 1X71 inverted epifluorescence microscope and Hamamatsu Orca 12-bit digital camera. Grey scale images were captured at excitation wavelengths of 480, 535 and 360 nm, emission wavelength of 535, 610 and 460 nm for Alexa Fluor® 488 fluorescence, DsRed fluorescence and DAPI florescence, respectively. Colors were applied to grey scale images using Adobe Photoshop™ software to represent the different emission colors: green for Alexa Fluor® 488, red for DsRed, and blue for DAPI. Regions of interest were defined using Compix SimplePCI™ software by outlining nonfluorescent cells or cells expressing DsRed fluorescence. Coverslips incubated without primary antibody had no detectable fluorescence with 490 nm excitation at the gain and exposure settings used. The specificities of the antibodies were confirmed as shown in Supplemental Figure 1.

3. Results

3.1 Knockdown of KCNQ5 channel subunits by KCNQ5shRNA in A7r5 cells

In our previous work, we established that 100 pM AVP induces a PKC-dependent suppression of KCNQ currents in A7r5 cells [4]. To more clearly establish that this function is mediated specifically by KCNQ5, which was the only member of the KCNQ family detected by RT-PCR in A7r5 cells [4], we knocked down KCNQ5 channels by infecting A7r5 cells with an adenoviral vector for bicistronic expression of KCNQ5shRNA and DsRed fluorescent marker.

Suppression of KCNQ5 channel protein was detected by immunofluorescence using rabbit polyclonal anti-KCNQ5 antibody. KCNQ5 immunofluorescence was invariably low in A7r5 cells expressing DsRed (Figure 1A), whereas control uninfected A7r5 cells often exhibited robust and in many cases punctuate immunofluorescence staining. The specificity of the KCNQ5 antibody was confirmed by the increased immunoflourescence in A7r5 cells overexpressing KCNQ5 and the absence of immunoreactivity when the primary antibody was omitted (Supplemental figure 1A). KCNQ currents measured by whole cell perforated patch clamp electrophysiology indicated that KCNQ5shRNA expression completely abolished KCNQ currents in A7r5 cells (Figure 1B and 1C).

3.2 KCNQ current suppression is a prominent mechanism for regulating Ca^{2+} spiking, but cannot fully account for the actions of AVP in A7r5 cells

To test our hypothesis that KCNQ current suppression regulates Ca^{2+} entry, we measured Ca^{2+} spiking responses in fura-2-loaded A7r5 cells expressing KCNQ5shRNA. In parallel cell cultures, spontaneous Ca^{2+} spikes were rarely observed in control cells (n=3) or scrambled shRNA-expressing cells (n=3), whereas expression of KCNQ5shRNA produced significantly greater repetitive spontaneous Ca^{2+} spiking activity (2.5 ± 0.5 spikes/min, n=6, $P<0.005$) (Figure 2A & 2B). The Ca^{2+} spiking frequency was increased significantly with the addition of 25pM AVP in KCNQ5shRNA-expressing A7r5 cells (compare KCNQ5shRNA bars in Figure 2 panels B and D; $p<0.05$). However the AVP-induced Ca^{2+} spiking frequency in KCNQ5shRNA-expressing A7r5 cells (5.0 ± 0.6 spikes/min) was not significantly different ($p>0.1$) from AVP-induced Ca^{2+} spiking in control cells (5.1 ± 0.4 spikes/min; n=10) or scrambled shRNA expressing cells (6.4 ± 0.7 spikes/min; n=3) (Figure 2D). A single Ca^{2+} spike generally occurred at the time of AVP injection, but this was likely a mechanically-induced transient because injection of control medium also induced an instantaneous spike, but did not produce repetitive Ca^{2+} spiking (results not shown). These observations indicate that K^+ conductance through KCNQ5 channels regulates Ca^{2+} entry in A7r5 cells. These results also indicate that, apart from KCNQ5 current suppression, AVP regulates Ca^{2+} spiking by some additional mechanism.

3.3 AVP-induced activation of TRPC6 in A7r5 cells

To explore the contribution of TRPC6 non-selective cation channels to the AVP-induced Ca^{2+} spiking response, A7r5 cells were infected with an adenoviral vector for bicistronic expression of TRPC6shRNA and DsRed fluorescent marker. TRPC6 channel protein was detected in the same cells by immunostaining with a polyclonal anti-TRPC6 antibody. Robust TRPC6 immunofluorescence was observed in uninfected A7r5 cells, whereas those expressing TRPC6shRNA had little detectable immunofluorescence (Figure 3A). The specificity of the TRPC6 antibody was confirmed by the loss of immunofluorescence when the TRPC6 antibody was pre-incubated with a TRPC6-specific blocking peptide (Supplemental figure 1B). The function of TRPC6 channels in A7r5 cells was evaluated by electrophysiological measurement of AVP-stimulated non-selective cation currents (I_{CAT}). I_{CAT} activation by 100 nM AVP was suppressed in all TRPC6shRNA-expressing cells (Figure 3B, 3C), with I_{CAT} activation reduced to undetectable levels in 7 of 13 such cells. Both outward and inward components of I_{CAT} were significantly reduced (by ~70% on average) in TRPC6shRNA-expressing cells (n=13) compared to non-fluorescent control cells (n=11, Figure 3D). In contrast, KCNQ5shRNA expression did not affect I_{CAT} current densities (Figure 3C, 3D).

3.4 KCNQ5 channel suppression is sufficient to induce membrane depolarization; TRPC6 channel knockdown does not affect resting membrane potential or AVP-induced membrane depolarization

Having previously proposed that PKC-dependent suppression of KCNQ channels contributes to AVP-induced Ca^{2+} spiking in A7r5 cells and AVP-induced mesenteric artery constriction [4,6], we chose to explore whether specifically suppressing KCNQ5 activity alone might be sufficient to induce membrane depolarization. KCNQ5shRNA-expressing A7r5 cells were significantly depolarized (−16 ± 4.1 mV; n=9, p<0.001) compared to uninfected control cells (−51.6 ± 1.9 mV; n=6) (Figure 4A). Addition of 100pM AVP induced additional depolarization (by 5.9 ± 1.1 mV; n=9, p<0.001) in KCNQ5shRNA-expressing A7r5 cells (Figure 4A). However, this additional AVP-induced depolarization in KCNQ5shRNA-expressing cells was significantly less than that in control A7r5 cells (9.8 ± 1.2 mV; n=6, p<0.05). Approximately 25% of cells expressing KCNQ5shRNA were spontaneously electrically active (repetitive action potential firing observed in 4 out of 16 cells; figure 4B); the remaining 75% of the cells examined were depolarized to such an extent that these cells did not show any spontaneous electrical activity. Neither resting potential nor the level of AVP-induced depolarization was significantly altered by TRPC6shRNA expression (Figure 4A).

3.5 TRPC6 expression determines the latency to AVP-induced Ca^{2+} spiking in A7r5 cells

We next chose to see whether the reduction of AVP-induced I_{CAT} in TRPC6shRNA-expressing cells (Figure 3D) would have any significance for the stimulation of Ca^{2+} spiking by physiological concentrations of AVP. Ca^{2+} spiking measurements in fura-2-loaded cells revealed that the latency to onset of Ca^{2+} spiking in TRPC6shRNA-expressing A7r5 cells was significantly greater than in control cells (13.2 ± 1.9 Vs. 7.8 ± 1.6 min; n=6 for each condition, p<0.005; Figure 5A and 5B). AVP-stimulated Ca^{2+} spiking was not observed during 25 min recordings in 4 out of the 18 wells plated with TRPC6shRNA-expressing A7r5 cells. In contrast, all the corresponding 18 wells plated with control A7r5 cells spiked normally. Interestingly, after initiation of Ca^{2+} spiking, the frequency of Ca^{2+} spiking in TRPC6shRNA-expressing cells was not different from control A7r5 cells (4.1 ± 0.6 Vs 4.5 ± 0.2 spikes/min; n=6 for each condition, p>0.1) (Figure 5C). In current-clamp recording, application of 100 pM AVP stimulated action potential (AP) firing in a substantial fraction of control A7r5 cells (observed in 9 out of 21 cells), whereas stimulation of AP firing by 100 pM AVP was not observed during similar recording periods in any cells expressing TRPC6shRNA (in 17 out of 17 cells, data not shown). These data further suggest that the mechanism of AVP-induced membrane depolarization is not limited to suppression of KCNQ channels alone, but also involves TRPC6 activation.

3.6 The role of DAG as a second messenger in AVP-stimulated Ca^{2+} spiking in A7r5 cells

Diacylglycerol (DAG) produced via breakdown of membrane phospholipids may contribute to both the PKC-dependent suppression of KCNQ5 currents and the activation of TRPC6 currents by AVP. To evaluate the relative ability of DAG to effect these downstream responses, we tested the effects of a membrane-permeant DAG analog, 1-oleoyl-2-acetyl-sn-glycerol (OAG), on KCNQ5 currents, I_{CAT} activation, and Ca^{2+} spiking. OAG (100 μM) significantly suppressed KCNQ5 currents at all voltages positive to −60 mV (p<0.05; Figure 6A and 6B) and stimulated Ca^{2+} spiking in A7r5 cells (Figure 6D). Both effects were abolished by a selective PKC inhibitor, Ro-31-8220 (2 μM) (Figure 6C and 6D). OAG also stimulated Ca^{2+} spiking in TRPC6shRNA-expressing A7r5 cells, but the latency to its onset was significantly increased when compared to control (19.4 ± 0.9 Vs. 17.7 ± 1.3 min; n=4 for each condition, P<0.05; Figure 6E). The frequency of OAG-induced Ca^{2+} spiking in TRPC6shRNA-expressing cells was not different from control A7r5 cells (6.3 ± 0.9 Vs 7.3 ± 0.6 spikes/min; n=4 for each condition, p>0.1; Figure 6F). These results suggest that despite its ability to

directly activate TRPC6 channels (Supplemental figure 2), DAG contributes to the stimulation of Ca^{2+} spiking primarily *via* PKC-dependent suppression of KCNQ5 currents.

3.7 Na^+-free medium eliminates inward I_{CAT} and reduces frequency/increases latency to AVP-stimulated Ca^{2+} spiking in A7r5 cells

To determine whether Na^+ influx through TRPC6 contributes to AVP-stimulated Ca^{2+} spiking, I_{CAT} and Ca^{2+} spiking were measured in Na^+-free conditions. Inward I_{CAT} activated by 1 nM AVP was abolished when Na^+ in the external solution was replaced with NMDG, an impermeant cation (Figure 7A). The latency to onset of Ca^{2+} spiking in A7r5 cells in Na^+-free medium was also significantly increased from that in control medium (16.6 ± 3.6 Vs 4.7 ± 1.0 min; n=4 for each condition; $p<0.05$, Figure 7B and 7C). The frequency of 25pM AVP-induced Ca^{2+} spiking in A7r5 cells in Na^+-free medium was significantly less than in cells maintained in Na^+-containing medium (3.5 ± 0.4 Vs 6.1 ± 0.6 spikes/min; n=4 for each condition, $p<0.01$, Figure 7B and 7D).

4. Discussion

Although the signal transduction of AVP in VSMCs has been studied for decades, there is still a paucity of information about the mechanisms of action of physiologically or therapeutically relevant concentrations of AVP. In the systemic circulation, concentrations of 100 pM or less are sufficient to produce a robust pressor response [20]. Most studies exploring AVP signal transduction pathways have utilized supraphysiological (nanomolar to micromolar) concentrations of AVP. Based on such studies, the actions of AVP on vascular smooth muscles cells are often attributed to the release of intracellular Ca^{2+} stores. There is nonetheless general recognition that voltage-sensitive Ca^{2+} channels (VSCC) also contribute to vasoconstrictor responses, but with little agreement as to the mechanisms whereby those channels may become activated. We previously elucidated a potential mechanism activated by physiological (picomolar) concentrations of AVP that leads to VSCC-dependent action potential firing in A7r5 vascular smooth muscle cells. We found that this process involves PKC-mediated suppression of KCNQ K^+ channel activity. KCNQ channel inhibition provides a depolarizing stimulus for activation of L-type VSCC. In the present study, we have investigated another mechanism by which AVP may depolarize vascular smooth muscle cells: activation of TRPC6 non-selective cation channels. Using a combination of molecular, electrophysiological, and cell physiological approaches, we provide evidence that specifically implicates both KCNQ5 and TRPC6 channels in the stimulation of Ca^{2+} spiking in VSMCs by physiological concentrations of AVP. Our results indicate that though suppression of KCNQ5 channels alone is sufficient to excite VSMCs, TRPC6 channel activation contributes to enhance excitation and Ca^{2+} entry in response to physiological concentrations of AVP.

4.1 Role of KCNQ currents as a determinant of resting membrane potential and Ca^{2+} spiking

Membrane potential of VSMCs controls Ca^{2+} influx through VSCC; membrane depolarization can lead to enhanced Ca^{2+} influx and vasoconstriction. Resting membrane potential is largely determined by K^+ conductance (G_K). This electrical conductance, which reflects the efflux of K^+ through channels that are active in unstimulated cells, maintains the resting membrane potential at very negative voltages that prevent opening of VSCC.

Of the many types of K^+ channels expressed in VSMCs, KCNQ channels are among the few that are thought to be appreciably active in unstimulated vascular myocytes [4,6]. The membrane resistance (R_m) of arterial smooth muscle cells is high, in the order of 5–15GΩ [21]. Hence even closure of a few channels that conduct K^+ at resting membrane potential would produce significant membrane depolarization. We found that knockdown of KCNQ5 in A7r5 cells shifted the membrane potential by +35mV, revealing an important contribution of

G_K through KCNQ channels at resting membrane potentials. This membrane depolarization (Figure 4A), was associated with spontaneous Ca^{2+} spiking (Figure 2A) and action potential firing (Figure 4B). These results complement the previous findings from our laboratory in which pharmacological suppression of KCNQ currents with linopirdine produced membrane depolarization, Ca^{2+} spiking, and action potential firing [4,6].

Expression of KCNQ channel subunits has been detected in a variety of arterial tissues or vascular myocytes: KCNQ1 in murine portal vein [13], KCNQ 1, 4 and 5 in mouse aorta, carotid artery, femoral artery and mesenteric artery [14], KCNQ5 in A7r5 rat aortic smooth muscle cells and KCNQ1 and 5 in rat aorta [4], KCNQ 1, 4 and 5 in rat mesenteric artery myocytes [6]. The function of KCNQ channels as negative regulators of vasoconstriction has been demonstrated recently in murine portal vein [22], pulmonary artery [23] and mesenteric artery [6]. It remains to be determined if KCNQ5 is the functionally predominant KCNQ subtype in all VSMCs. Further studies to elucidate the expression and function of KCNQ family of channels in various vascular beds will greatly enhance our understanding of their role in regulation of blood vessel diameter.

4.2 Response to a physiological concentration of AVP involves additional mechanisms apart from KCNQ5 current suppression: TRPC6 channels contribute to elevate $[Ca^{2+}]_i$ in response to a physiological concentration of AVP

The L-type Ca^{2+} channel-dependent Ca^{2+} spiking observed at low concentrations of AVP [24] is different from the IP_3-mediated Ca^{2+} release oscillations observed in A7r5 cells [25] or rat hepatocytes [26] treated with nanomolar concentrations of AVP. Supra-physiological (nanomolar to micromolar) concentrations of AVP activate PLC and subsequently induce IP_3-mediated Ca^{2+} release from the sarcoplasmic reticulum [3,27,28]. In some cells, repetitive cycles of Ca^{2+} release and reuptake are exhibited as oscillations in $[Ca^{2+}]_i$ [25,26]. However, unlike the Ca^{2+} spiking responses, the Ca^{2+} release oscillations are resistant to L-type Ca^{2+} channel blockers. Furthermore, at physiological concentrations (≤100pM) of AVP the Ca^{2+} release responses in A7r5 cells are barely detectable [24,29]. Suppression of KCNQ5 currents, leading to membrane depolarization and Ca^{2+} entry through voltage-sensitive Ca^{2+} channels, may provide a different Ca^{2+} signaling mechanism by which physiological [AVP] can exert its vasoconstrictor actions [4,6].

Signal transduction mechanisms activated at picomolar concentrations of AVP have rarely been examined and therefore it is unclear whether suppression of KCNQ channels is the only downstream target of V_{1a} vasopressin receptor activation in the physiological concentration range. In KCNQ5shRNA-expressing cells with no detectable KCNQ currents (Figure 1B), addition of a physiological concentration of AVP (100pM) produced a significant additional depolarization (Figure 4A) and increase in Ca^{2+} spiking frequency (Figure 2D), suggesting that additional signaling elements do contribute to these functional responses. The extent of depolarization is greater with KCNQ5 knockdown (compared to AVP-induced depolarization), but Ca^{2+} spiking is more robust with AVP treatment. With AVP treatment, suppression of KCNQ5 currents is combined with an increase in inward current (e.g. through activation of TRPC6 channels). This may be expected to increase the rate of depolarization and hence the frequency of firing compared with even more complete suppression of KCNQ5 current alone, because in the latter case only the resting inward current (leak current) provides the depolarizing stimulus.

While a 10–100 pM concentration of AVP produced a Ca^{2+} spiking response, these concentrations did not stimulate an appreciable release of intracellular Ca^{2+} stores [24] and hence it is unlikely that store-operated currents (I_{soc}) play a significant role in Ca^{2+} entry at these concentrations of AVP. Hence we chose to explore the contribution of the non-selective cation current (I_{CAT}) to 25pM AVP-stimulated Ca^{2+} responses.

Members of the transient receptor potential (TRP) family of non-selective cation channels have been implicated as targets for vasoconstrictor signal transduction [30,31]. Expression of TRPC1, 4, 6 and 7 of the classical TRP channel subfamily (TRPC) has been reported in A7r5 cells [17,18,32,33]. TRPC1 is a candidate store-operated channel or part of the store operated channel in VSMCs, including A7r5 cells [32,34,35]. TRPC4 channels have also been recently reported to mediate store operated Ca^{2+} entry in VSMCs [36]. TRPC6 and TRPC7 are members of the DAG-sensitive TRPC subgroup (TRPC3/6/7) [37,38], of which TRPC6 channels have been proposed as candidate receptor-operated channels in A7r5 cells [17,18]. TRPC6 channels, which have low selectivity for Ca^{2+} over Na^{+} [39,40], can increase $[Ca^{2+}]_i$ via at least 3 mechanisms: 1) the influx of cations through TRPC6 channels would shift the membrane potential to more positive values to activate VSCC; 2) influx of Na^{+} through TRPC6 channels may result in elevated cytosolic Na^{+} concentration and increase $[Ca^{2+}]_i$ by reversing the Na^{+}/Ca^{2+}-exchanger (NCX) [41]; 3) influx of Ca^{2+} directly through TRPC6 channels may contribute to elevate $[Ca^{2+}]_i$. Previous efforts to evaluate the contributions of TRPC6 in AVP signaling have focused on effects induced by maximal [AVP] (100nM), which produces a robust Ca^{2+} release and influx of Ca^{2+} [17,18], but may not be relevant for more physiological concentrations of AVP.

In our studies, knockdown of TRPC6 reduced AVP-stimulated I_{CAT} by ~70% (Figure 3D), indicating that TRPC6 is the principal non-selective cation channel stimulated by AVP. These results also confirm that endogenous TRPC6 is the major mediator of I_{CAT} in A7r5 cells [17, 18]. Examination of Ca^{2+} spiking responses to physiological concentrations of AVP in A7r5 cells, showed that knockdown of TRPC6 produced a shift in latency to onset of spiking but did not alter the frequency of spiking in response to 25pM AVP (Figure 5). Furthermore, knockdown of TRPC6 did not alter the resting membrane potential or depolarization in response to AVP (Figure 4A). These results suggest that I_{CAT} through TRPC6 contributes only modestly to membrane potential when KCNQ channels are open. However when KCNQ channel activity is suppressed by physiological [AVP], membrane resistance (R_m) increases [4]. According to Ohm's law [Voltage (V) = Current (I) × Resistance (R)], when the resistance is high, even a small increase in I_{CAT} through TRPC6 will be able to depolarize the VSMC more effectively. Hence the influx of cations through TRPC6 channels might be sufficient to more rapidly attain the threshold to activate VSCC and trigger firing of Ca^{2+}-dependent action potentials (AP).

In a previous study, OAG-induced Ca^{2+} entry in A7r5 cells was abolished by nimodipine, a blocker of L-type Ca^{2+} channels, suggesting a membrane depolarizing effect of the DAG analog [18]. The authors of that study concluded that OAG-induced Ca^{2+} entry was a result of membrane depolarization (via activation of TRPC6 and enhanced cation influx) and activation of L-type Ca^{2+} channels. However, in the same study, knockdown of TRPC6 in A7r5 cells did not prevent Ca^{2+} entry induced by application of OAG (100 μM) [18]. We found that, although 100 μM OAG activated I_{CAT} (Supplemental Figure 2) as observed in the previous study, it also significantly suppressed KCNQ5 currents in A7r5 cells (Figure 6A and 6B). TRPC6shRNA expression only increased the latency to onset of OAG-induced Ca^{2+} spiking, but, inhibition of PKC completely abolished OAG-induced Ca^{2+} spiking (Figure 6D). Inhibition of PKC had no effect on OAG-activated TRPC6 currents [16] and in general, PKC activation is thought to inhibit rather than activate TRPC channels [42]. If Ca^{2+} spiking were caused primarily by TRPC6 activation, PKC inhibition would enhance rather than inhibit Ca^{2+} spiking. Hence AVP-stimulated Ca^{2+} spiking can more reasonably be attributed to DAG-induced PKC activation and suppression of KCNQ currents. It is also likely that the OAG-stimulated Ca^{2+} entry in the previous study [18] might have involved PKC-dependent suppression of KCNQ channel activity rather than activation of TRPC6 alone.

Knockdown of TRPC6 channels in A7r5 cells shifted the latency to onset of Ca^{2+} spiking, but did not alter the frequency of spiking in response to 25pM AVP (Figure 5). However in Na^+-free conditions both the latency to onset of spiking and frequency of spiking were changed (Figure 7). This raises the possibility that there might be some contribution from other Na^+-conducting pathways that influences spike frequency.

A functional coupling of TRPC6 and Na^+/Ca^{2+} exchanger (NCX) has been proposed for rat aortic smooth muscle cells [41,44,45]. While purinergic receptor stimulation produced reversal of the NCX to mediate Ca^{2+} influx, it remains to be seen whether the same mechanism also contributes to AVP-induced Ca^{2+} influx. The contribution of Ca^{2+} influx directly though TRPC6 is likely to be small because the selectivity of TRPC6 channels for Ca^{2+} is very low compared to Na^+ [39,40,46].

Studies to understand the physiological role of TRPC6 channels remain a significant challenge because selective TRPC6 channel blockers and activators are not yet available. The picture is complicated further because TRPC6 is known to interact with other members of the DAG-responsive TRPC subfamily, TRPC3 and TRPC7, to form tetrameric channels [33,37]. In A7r5 cells, TRPC6 was found to interact with TRPC7. Hence it is highly likely that TRPC6 exists as a heteromultimer in vascular smooth muscle with TRPC3, TRPC7 or perhaps other members of the TRPC family. Nonetheless, we and others [18] have found that knocking down TRPC6 expression in A7r5 cells results in a dramatic reduction of AVP-stimulated non-selective cation currents. Our present findings further suggest that activation of TRPC6-mediated Na^+ entry contributes to the Ca^{2+} responses of VSMCs to physiological concentrations of AVP.

4.3 Hypothetical signal transduction pathway for AVP-stimulated Ca^{2+} spiking in vascular smooth muscle cells

We propose that at physiological concentrations, AVP signal transduction involves production of diacylglycerol (DAG), presumably by activation of phospholipases D and C (PLD and PLC) [47]. DAG-induced PKC activation causes suppression of KCNQ5 channel-mediated K^+ efflux and robust membrane depolarization that results in Ca^{2+} influx through voltage-sensitive Ca^{2+} channels. Increased concentrations of DAG, apart from activating PKC, also directly activate TRPC6 channels. Na^+ and Ca^{2+} influx through TRPC6 channels contribute modestly to membrane depolarization, but this contribution is sufficient to enhance the membrane depolarization produced by suppression of KCNQ5 currents. This reduces the time required to reach the membrane potential threshold for activation of voltage-sensitive Ca^{2+} channels and Ca^{2+} influx. Ca^{2+} influx through TRPC6 and reversal of Na^+/Ca^{2+} exchange following influx of Na^+ may also modestly contribute to the robust increase in $[Ca^{2+}]_i$ through the voltage-sensitive Ca^{2+} channels (Figure 8).

5. Conclusions

In summary, from the present study we conclude that (1) KCNQ5 channels conduct K^+ at resting membrane potentials in A7r5 cells. The resulting outward K^+ current opposes membrane depolarization and prevents E_m from reaching the threshold for triggering action potential firing; (2) Suppression of KCNQ5 channel activity by physiological concentrations of AVP will depolarize the membrane and stimulate Ca^{2+} influx though voltage-sensitive Ca^{2+} channels; (3) Activation of TRPC6 non-selective cation currents modestly contributes to AVP-induced membrane depolarization and generation of Ca^{2+} spikes at physiological concentrations of AVP.

Supplementary Material

Refer to Web version on PubMed Central for supplementary material.

Acknowledgments

This work was supported by the National Heart Lung & Blood Institute (R01 HL070670 to KLB)

The authors gratefully acknowledge the technical support of Chris Hill.

References

1. Holmes CL, Landry DW, Granton JT. Science review: Vasopressin and the cardiovascular system part 1--receptor physiology. Crit Care 2003;7:427–34. [PubMed: 14624682]
2. Thibonnier M, Bayer AL, Simonson MS, Kester M. Multiple signaling pathways of V1-vascular vasopressin receptors of A7r5 cells. Endocrinology 1991;129:2845–56. [PubMed: 1659517]
3. Nemenoff RA. Vasopressin signaling pathways in vascular smooth muscle. Front Biosci 1998;3:d194–207. [PubMed: 9456345]
4. Brueggemann LI, Moran CJ, Barakat JA, Yeh JZ, Cribbs LL, Byron KL. Vasopressin stimulates action potential firing by protein kinase C-dependent inhibition of KCNQ5 in A7r5 rat aortic smooth muscle cells. Am J Physiol Heart Circ Physiol 2007;292:H1352–63. [PubMed: 17071736]
5. Henderson KK, Byron KL. Vasopressin-induced vasoconstriction: two concentration-dependent signaling pathways. J Appl Physiol 2007;102:1402–9. [PubMed: 17204577]
6. Mackie AR, Brueggemann LI, Henderson KK, et al. Vascular KCNQ potassium channels as novel targets for the control of mesenteric artery constriction: based on studies in single cells, pressurized arteries and in vivo measurements of mesenteric vascular resistance. J Pharmacol Exp Ther 2008;325:475–483. [PubMed: 18272810]
7. Parrillo JE. Septic shock--vasopressin, norepinephrine, and urgency. N Engl J Med 2008;358:954–6. [PubMed: 18305271]
8. Lemmens-Gruber R, Kamyar M. Vasopressin antagonists. Cell Mol Life Sci 2006;63:1766–79. [PubMed: 16794787]
9. Ali F, Guglin M, Vaitkevicius P, Ghali JK. Therapeutic potential of vasopressin receptor antagonists. Drugs 2007;67:847–58. [PubMed: 17428103]
10. Wang HS, Pan Z, Shi W, et al. KCNQ2 and KCNQ3 potassium channel subunits: molecular correlates of the M-channel. Science 1998;282:1890–3. [PubMed: 9836639]
11. Delmas P, Brown DA. Pathways modulating neural KCNQ/M (K_V7) potassium channels. Nat Rev Neurosci 2005;6:850–62. [PubMed: 16261179]
12. Brown DA. Kv7 (KCNQ) potassium channels that are mutated in human diseases. J Physiol 2008;586:1781–3. [PubMed: 18381340]
13. Ohya S, Sergeant GP, Greenwood IA, Horowitz B. Molecular variants of KCNQ channels expressed in murine portal vein myocytes: a role in delayed rectifier current. Circ Res 2003;92:1016–23. [PubMed: 12690036]
14. Yeung SY, Pucovsky V, Moffatt JD, et al. Molecular expression and pharmacological identification of a role for K_V7 channels in murine vascular reactivity. Br J Pharmacol 2007;151:758–70. [PubMed: 17519950]
15. Marrion NV. Control of M-current. Annu Rev Physiol 1997;59:483–504. [PubMed: 9074774]
16. Hofmann T, Obukhov AG, Schaefer M, Harteneck C, Gudermann T, Schultz G. Direct activation of human TRPC6 and TRPC3 channels by diacylglycerol. Nature 1999;397:259–63. [PubMed: 9930701]
17. Jung S, Strotmann R, Schultz G, Plant TD. TRPC6 is a candidate channel involved in receptor-stimulated cation currents in A7r5 smooth muscle cells. Am J Physiol Cell Physiol 2002;282:C347–59. [PubMed: 11788346]
18. Soboloff J, Spassova M, Xu W, He LP, Cuesta N, Gill DL. Role of endogenous TRPC6 channels in Ca^{2+} signal generation in A7r5 smooth muscle cells. J Biol Chem 2005;280:39786–94. [PubMed: 16204251]
19. Byron KL, Taylor CW. Spontaneous Ca^{2+} spiking in a vascular smooth muscle cell line is independent of the release of intracellular Ca2+ stores. J Biol Chem 1993;268:6945–52. [PubMed: 8463226]

20. Holmes CL, Patel BM, Russell JA, Walley KR. Physiology of vasopressin relevant to management of septic shock. Chest 2001;120:989–1002. [PubMed: 11555538]
21. Nelson MT, Quayle JM. Physiological roles and properties of potassium channels in arterial smooth muscle. Am J Physiol 1995;268:C799–822. [PubMed: 7733230]
22. Yeung SY, Greenwood IA. Electrophysiological and functional effects of the KCNQ channel blocker XE991 on murine portal vein smooth muscle cells. Br J Pharmacol 2005;146:585–95. [PubMed: 16056238]
23. Joshi S, Balan P, Gurney AM. Pulmonary vasoconstrictor action of KCNQ potassium channel blockers. Respir Res 2006;7:31. [PubMed: 16504007]
24. Byron KL. Vasopressin stimulates Ca^{2+} spiking activity in A7r5 vascular smooth muscle cells via activation of phospholipase A2. Circ Res 1996;78:813–20. [PubMed: 8620601]
25. Li M, Zacharia J, Sun X, Wier WG. Effects of siRNA knock-down of TRPC6 and InsP(3)R1 in vasopressin-induced Ca(2+) oscillations of A7r5 vascular smooth muscle cells. Pharmacol Res 2008;58:308–15. [PubMed: 18835357]
26. Jones BF, Boyles RR, Hwang SY, Bird GS, Putney JW. Calcium influx mechanisms underlying calcium oscillations in rat hepatocytes. Hepatology 2008;48:1273–81. [PubMed: 18802964]
27. Thibonnier M. Signal transduction of V1-vascular vasopressin receptors. Regul Pept 1992;38:1–11. [PubMed: 1533467]
28. Van Renterghem C, Romey G, Lazdunski M. Vasopressin modulates the spontaneous electrical activity in aortic cells (line A7r5) by acting on three different types of ionic channels. Proc Natl Acad Sci U S A 1988;85:9365–9. [PubMed: 2461570]
29. Byron K, Taylor CW. Vasopressin stimulation of Ca2+ mobilization, two bivalent cation entry pathways and Ca2+ efflux in A7r5 rat smooth muscle cells. J Physiol 1995;485(Pt 2):455–68. [PubMed: 7666368]
30. Inoue R, Hai L, Honda A. Pathophysiological implications of transient receptor potential channels in vascular function. Curr Opin Nephrol Hypertens 2008;17:193–8. [PubMed: 18277154]
31. Brayden JE, Earley S, Nelson MT, Reading S. Transient Receptor Potential (Trp) Channels, Vascular Tone and Autoregulation of Cerebral Blood Flow. Clin Exp Pharmacol Physiol 2008;35:1116–1120. [PubMed: 18215190]
32. Brueggemann LI, Markun DR, Henderson KK, Cribbs LL, Byron KL. Pharmacological and electrophysiological characterization of store-operated currents and capacitative Ca^{2+} entry in vascular smooth muscle cells. J Pharmacol Exp Ther 2006;317:488–99. [PubMed: 16415091]
33. Maruyama Y, Nakanishi Y, Walsh EJ, Wilson DP, Welsh DG, Cole WC. Heteromultimeric TRPC6-TRPC7 channels contribute to arginine vasopressin-induced cation current of A7r5 vascular smooth muscle cells. Circ Res 2006;98:1520–7. [PubMed: 16690880]
34. Sweeney M, Yu Y, Platoshyn O, Zhang S, McDaniel SS, Yuan JX. Inhibition of endogenous TRP1 decreases capacitative Ca^{2+} entry and attenuates pulmonary artery smooth muscle cell proliferation. Am J Physiol Lung Cell Mol Physiol 2002;283:L144–55. [PubMed: 12060571]
35. Xu SZ, Beech DJ. TrpC1 is a membrane-spanning subunit of store-operated Ca^{2+} channels in native vascular smooth muscle cells. Circ Res 2001;88:84–7. [PubMed: 11139478]
36. Zhang S, Remillard CV, Fantozzi I, Yuan JX. ATP-induced mitogenesis is mediated by cyclic AMP response element-binding protein-enhanced TRPC4 expression and activity in human pulmonary artery smooth muscle cells. Am J Physiol Cell Physiol 2004;287:C1192–201. [PubMed: 15229105]
37. Dietrich A, Kalwa H, Rost BR, Gudermann T. The diacylgylcerol-sensitive TRPC3/6/7 subfamily of cation channels: functional characterization and physiological relevance. Pflugers Arch 2005;451:72–80. [PubMed: 15971081]
38. Ramsey IS, Delling M, Clapham DE. An introduction to TRP channels. Annu Rev Physiol 2006;68:619–47. [PubMed: 16460286]
39. Estacion M, Sinkins WG, Jones SW, Applegate MA, Schilling WP. Human TRPC6 expressed in HEK 293 cells forms non-selective cation channels with limited Ca2+ permeability. J Physiol 2006;572:359–77. [PubMed: 16439426]
40. Pedersen SF, Owsianik G, Nilius B. TRP channels: an overview. Cell Calcium 2005;38:233–52. [PubMed: 16098585]

41. Lemos VS, Poburko D, Liao CH, Cole WC, van Breemen C. Na+ entry via TRPC6 causes Ca^{2+} entry via NCX reversal in ATP stimulated smooth muscle cells. Biochem Biophys Res Commun 2007;352:130–4. [PubMed: 17112478]

42. Venkatachalam K, Zheng F, Gill DL. Control of TRPC and store-operated channels by protein kinase C. Novartis Found Symp 2004;258:172–85. [PubMed: 15104182]discussion 185–8, 263–6

43. Fan J, Byron KL. Ca^{2+} signalling in rat vascular smooth muscle cells: a role for protein kinase C at physiological vasoconstrictor concentrations of vasopressin. J Physiol 2000;524:821–31. [PubMed: 10790161]

44. Syyong HT, Poburko D, Fameli N, van Breemen C. ATP promotes NCX-reversal in aortic smooth muscle cells by DAG-activated Na^{+} entry. Biochem Biophys Res Commun 2007;357:1177–82. [PubMed: 17466270]

45. Poburko D, Liao CH, Lemos VS, et al. Transient receptor potential channel 6-mediated, localized cytosolic [Na^{+}] transients drive Na^{+}/Ca^{2+} exchanger-mediated Ca^{2+} entry in purinergically stimulated aorta smooth muscle cells. Circ Res 2007;101:1030–8. [PubMed: 17872462]

46. Dietrich A, Gudermann T. Trpc6. Handb Exp Pharmacol 2007:125–41. [PubMed: 17217054]

47. Li Y, Shiels AJ, Maszak G, Byron KL. Vasopressin-stimulated Ca^{2+} spiking in vascular smooth muscle cells involves phospholipase D. Am J Physiol Heart Circ Physiol 2001;280:H2658–64. [PubMed: 11356622]

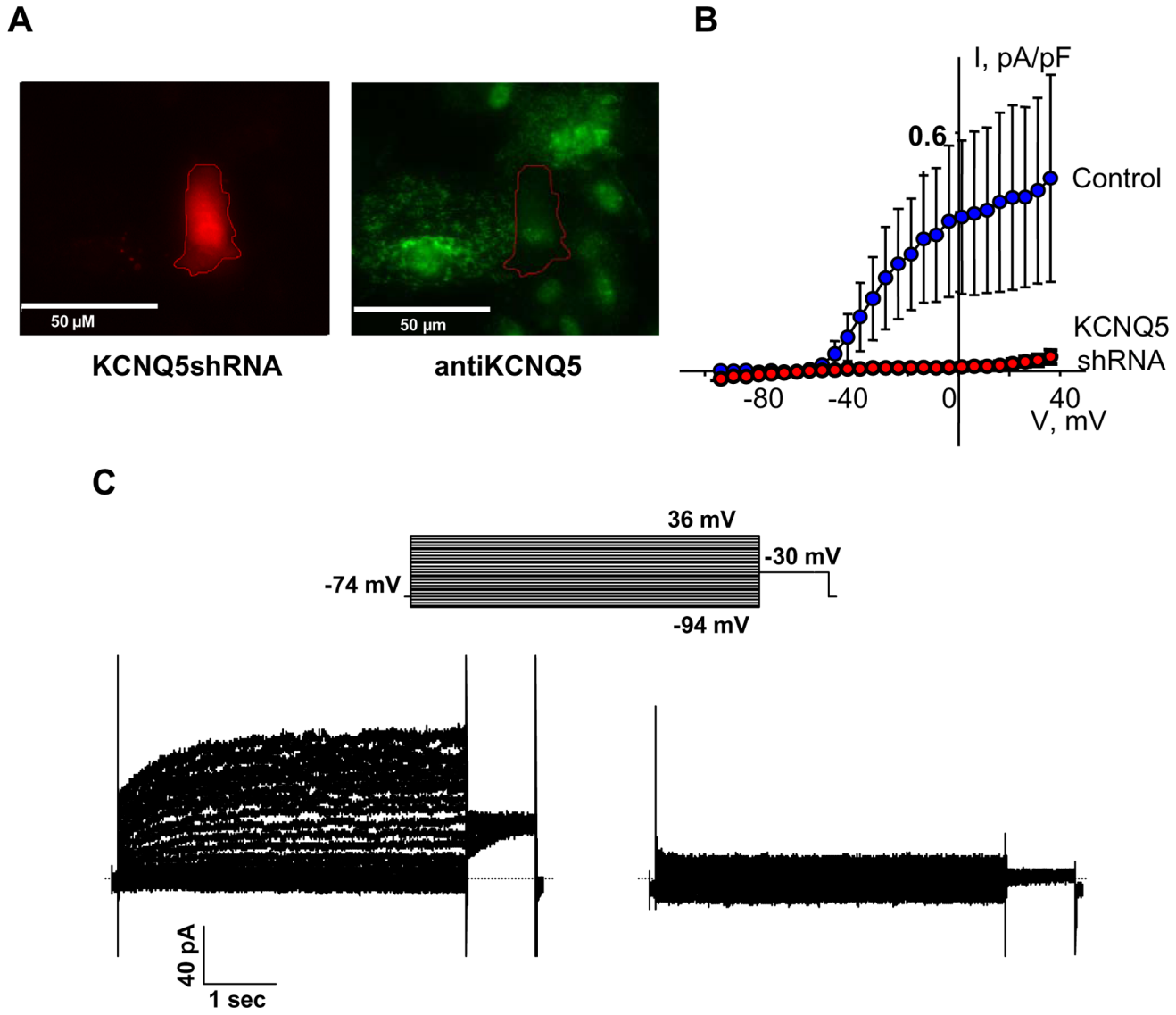

Figure 1. Expression of KCNQ5shRNA knocks down KCNQ5 channel protein and completely inhibits KCNQ currents in A7r5 cells

A. Left panel shows a representative cell expressing DsRed fluorescence when infected with a bicistronic adenoviral vector for expression of KCNQ5shRNA and DsRed fluorescent marker. Right panel shows anti-KCNQ5 immunofluorescence of the same field of cells. B. IV graph shows KCNQ currents measured in control A7r5 cells (blue circles, n=7) and in A7r5 cells expressing KCNQ5shRNA (red circles, n=8). I, current; *V*, voltage. Currents in A7r5 cells expressing KCNQ5shRNA were significantly smaller than control currents at all voltages positive to −49 mV ($p < 0.05$, Rank Sum test). C. Representative KCNQ current traces recorded from a control cell (uninfected, capacitance =189.5 pF, left) and a cell expressing KCNQ5shRNA (capacitance = 208.5 pF, right).

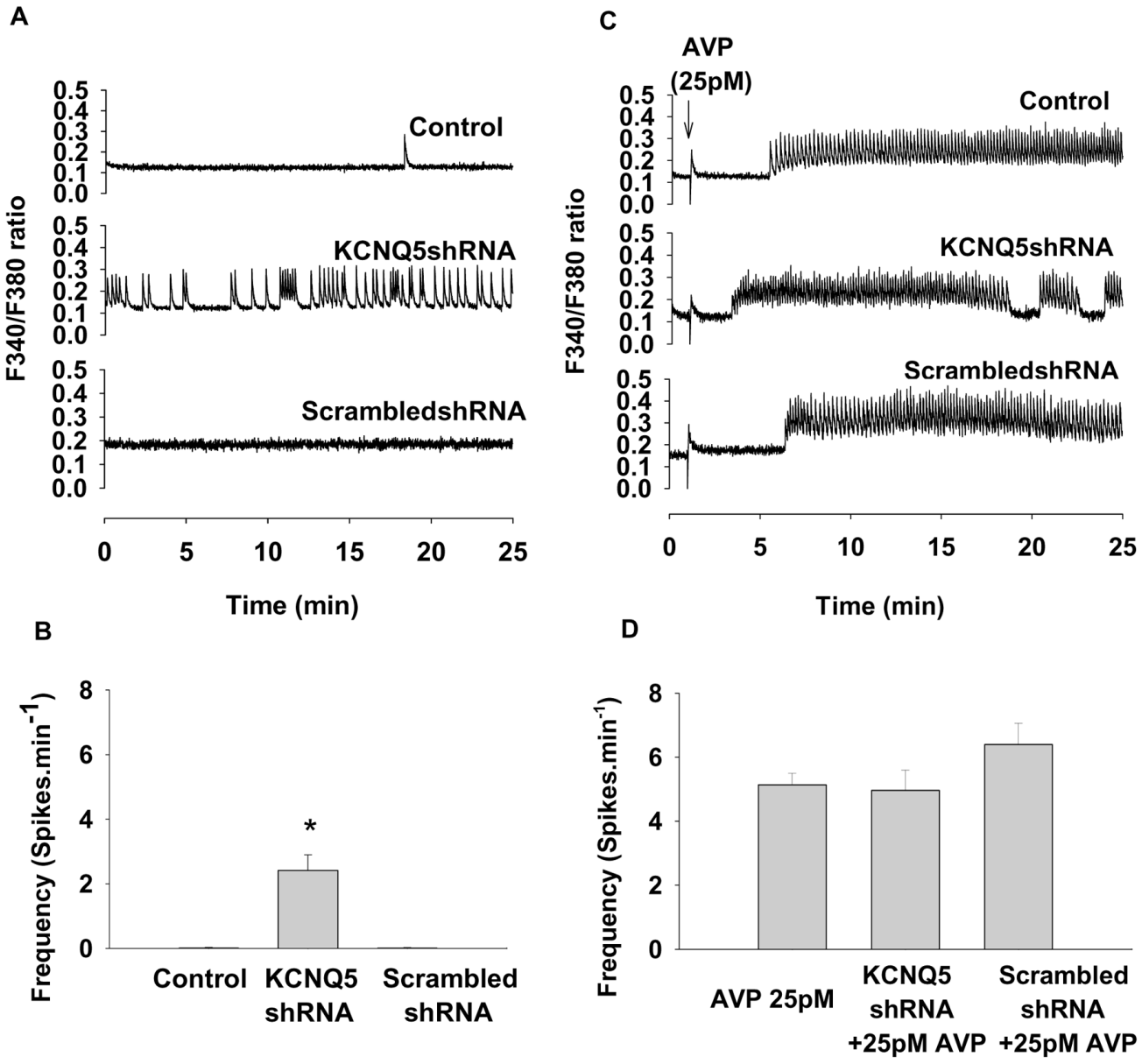

Figure 2. Spontaneous Ca^{2+} spiking is increased by KCNQ5 knockdown or by AVP treatment, but AVP is more effective

A. Representative time course of Ca^{2+} spiking in uninfected control A7r5 cells, cells expressing KCNQ5shRNA or scrambled shRNA. B. Bar graph shows Ca^{2+} spiking frequency in uninfected control A7r5 cells (n=3), cells expressing KCNQ5shRNA (n=6) or scrambled shRNA (n=3). *Statistically significant difference from both scrambled shRNA and uninfected controls (p<0.005, one-way ANOVA followed by Holm-Sidak post hoc method). C. Representative time course of Ca^{2+} spiking with addition of 25pM AVP in uninfected control cells, cells expressing KCNQ5shRNA, or cells expressing scrambled shRNA. D. Bar graph shows Ca^{2+} spiking frequency with the addition of 25pM AVP in uninfected control cells (n=3), cells expressing KCNQ5shRNA (n=6), or scrambled shRNA (n=3). Differences between Ca^{2+} spiking frequency in AVP-treated KCNQ5shRNA, scrambled shRNA-expressing cells, and uninfected control cells were not statistically significant (p>0.1, one-way ANOVA).

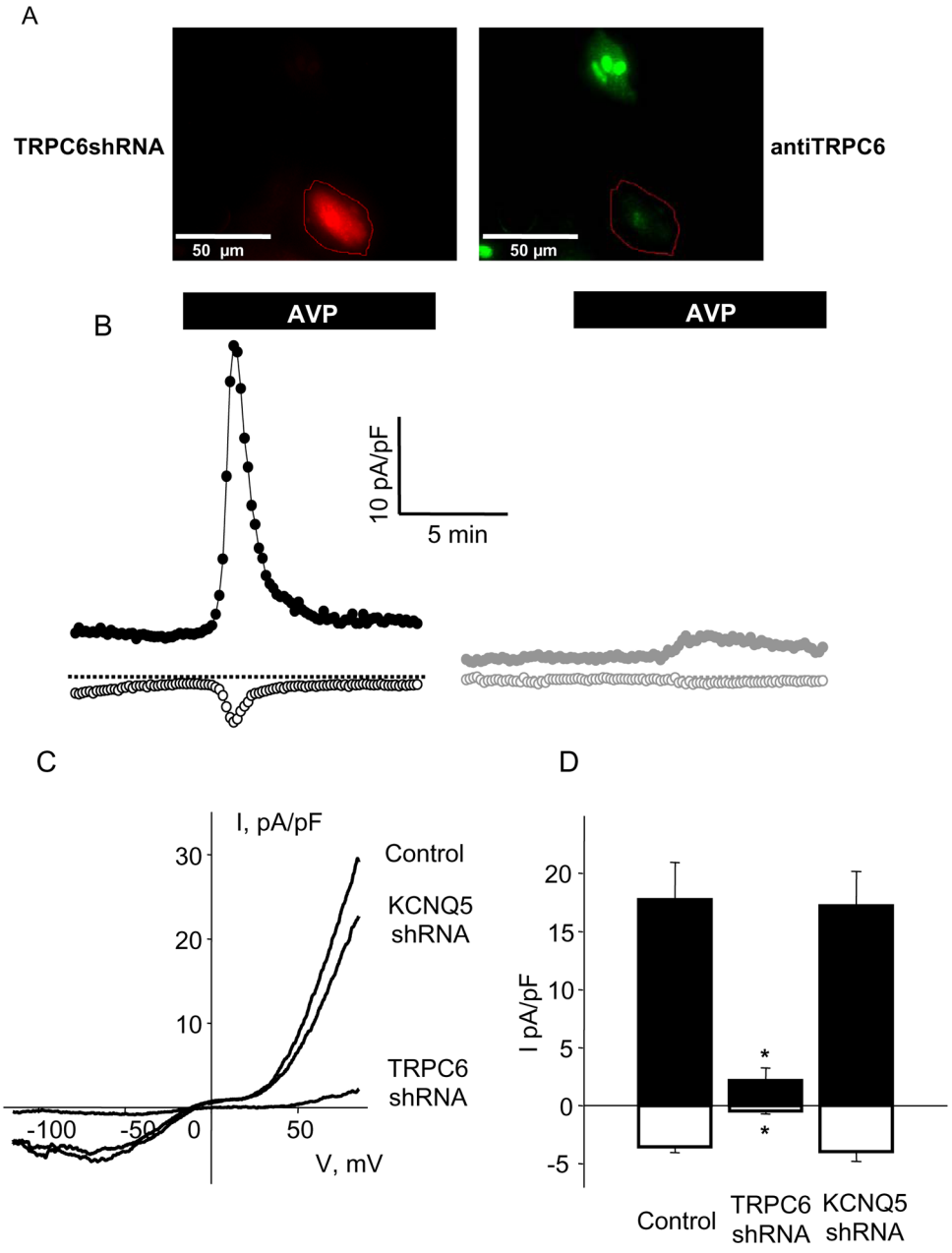

Figure 3. Expression of TRPC6shRNA reduced anti-TRPC6 immunoreactivity and caused suppression of AVP-induced I_{CAT} in A7r5 cells

A. Left panel shows a representative cell expressing DsRed fluorescence when infected with a bicistronic adenoviral vector for expression of TRPC6shRNA and DsRed fluorescent marker. Right panel shows anti-TRPC6 immunofluorescence of the same field of cells. B. Representative time course of I_{CAT} activation (outward currents shown by filled circles and inward currents shown by open circles) by 100 nM AVP in control (left panel) and TRPC6shRNA-expressing cells (right panel). C. Representative IV curves of AVP-induced I_{CAT} recorded in a control cell and a cell expressing TRPC6shRNA or KCNQ5shRNA. D. Bar graph shows AVP-induced I_{CAT} current density - outward currents (filled bars) measured at +85 mV and inward currents (open bars) measured at −115 mV in control cells (n=11), and

cells expressing TRPC6shRNA (n=13) or KCNQ5shRNA (n=4). *AVP-induced I_{CAT} was significantly reduced in TRPC6shRNA-expressing cells compared with control and KCNQ5shRNA-expressing cells ($p<0.05$ for outward current and $p<0.01$ for inward current, one-way ANOVA followed by Holm-Sidak post hoc method).

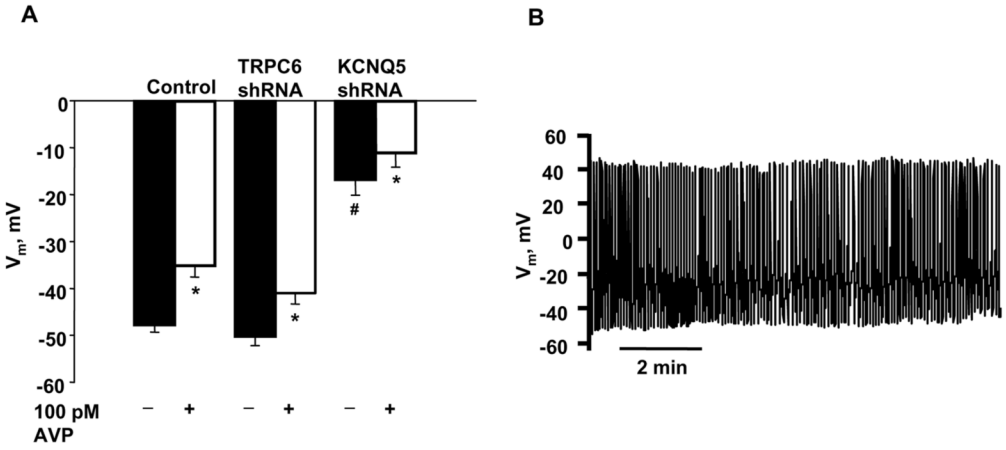

Figure 4. Knockdown of KCNQ5 channel depolarized A7r5 cells, but AVP induced further depolarization

A. Membrane potentials measured in current clamp mode in control A7r5 cells (black bar, n=6) and in cells expressing either TRPC6shRNA (dark grey bar, n=6) or KCNQ5shRNA (light grey bar, n=9); average values recorded for 5 min before application of 100 pM AVP (filled bars) and during the last 5 min of a 15 min AVP application (open bars). $^{\#}p<0.001$, statistically significant difference in resting membrane potential compared to TRPC6shRNA-expressing cells and control cells (one-way ANOVA followed by Holm-Sidak post hoc method); $^{*}p<0.001$, statistically significant difference with 100pM AVP treatment in all 3 groups (compared with untreated cells; Student's paired 't' test). B. Representative trace of membrane potential (V_m) recorded in current-clamp mode shows spontaneous electrical activity in a cell expressing KCNQ5shRNA.

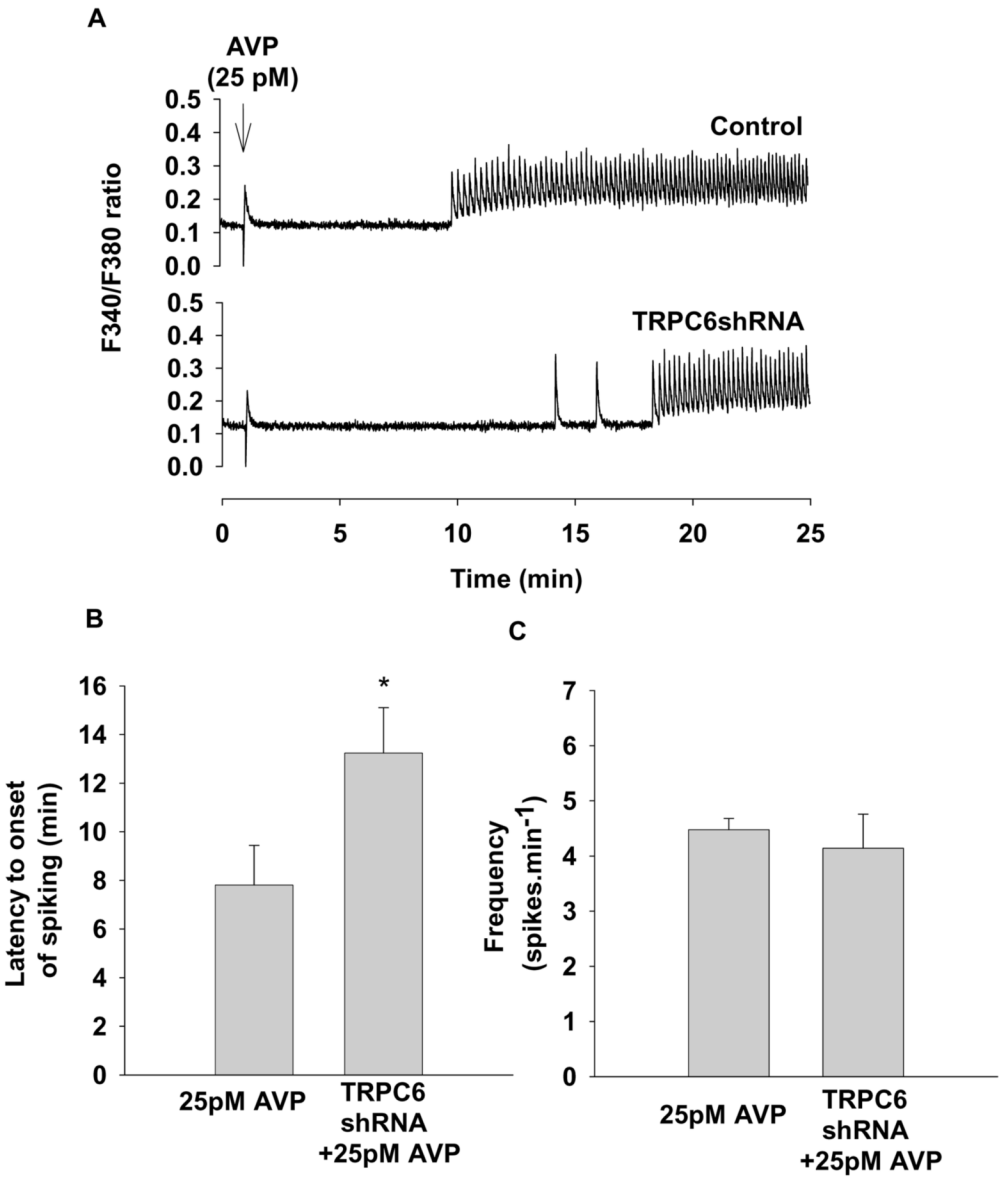

Figure 5. Knockdown of TRPC6 increases the latency to onset of AVP-induced Ca^{2+} spiking in A7r5 cells

A. Representative time course of 25pM AVP-induced Ca^{2+} spiking in control and TRPC6shRNA-expressing A7r5 cells. B. Bar graph shows the latency to onset of Ca^{2+} spiking in control and TRPC6shRNA-expressing A7r5 cells. *Statistically significant difference compared to control ($p<0.005$, Student's paired 't' test; n=6, for each condition). C. Bar graph shows the frequency of Ca^{2+} spiking in control and TRPC6shRNA-expressing A7r5 cells. No significant difference from control ($p>0.1$, Student's paired 't' test; n=6, for each condition).

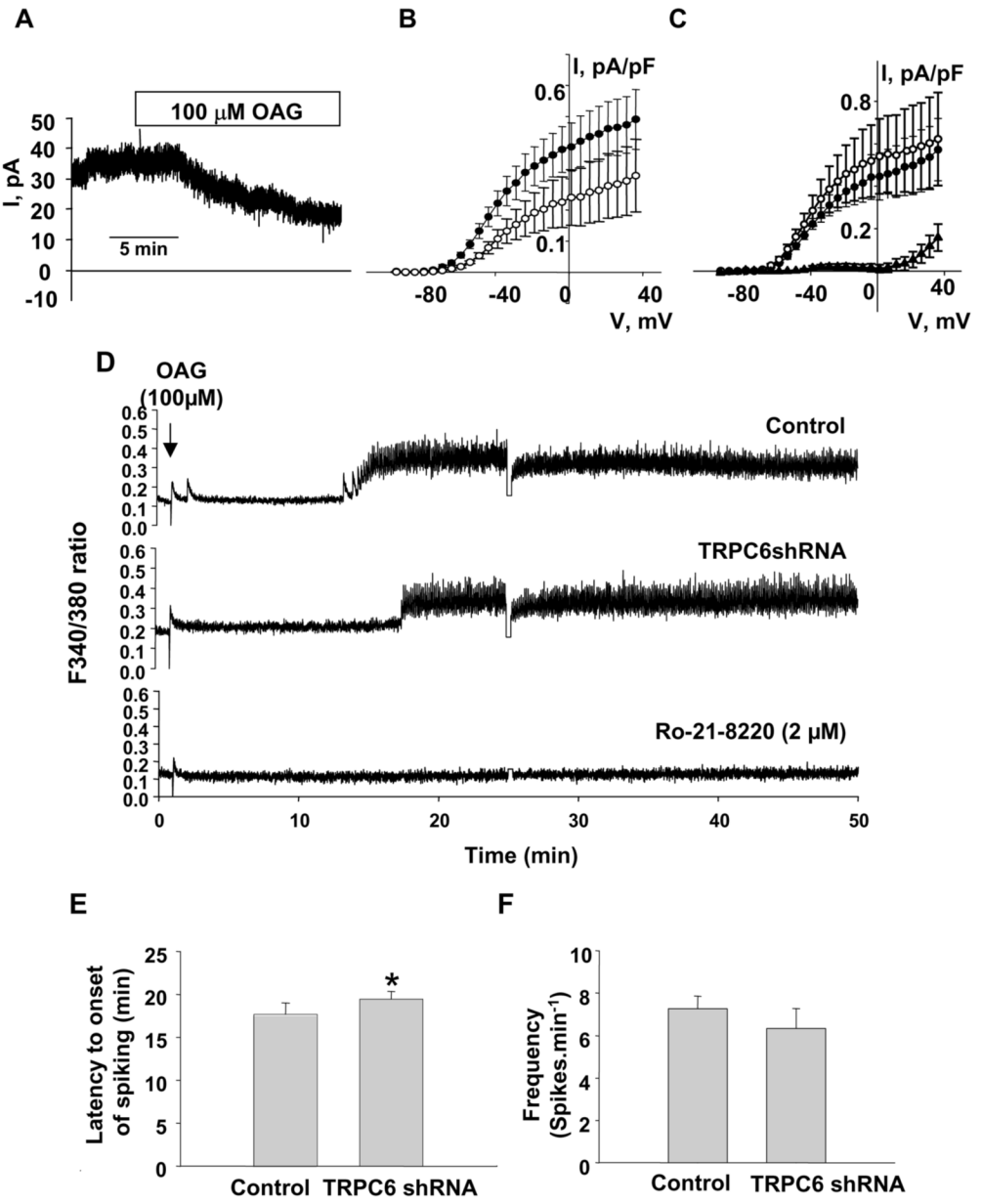

Figure 6. OAG-induced Ca^{2+} spiking involves TRPC6 channels, but requires PKC-dependent suppression of KCNQ5 currents

A. Representative KCNQ5 current trace recorded at −20 mV holding potential shows the time course of suppression of the currents with application of 100 μM OAG. B. IV curves of the KCNQ5 currents shows significant suppression of KCNQ5 currents by 100 μM OAG at all voltages positive of −60 mV (p<0.05, Student's paired 't' test; n=4). C. IV curve shows a 1-hr pretreatment with 2 μM Ro-31-8220 prevented OAG-induced suppression of KCNQ5 current (no difference from control, p>0.1, Student's paired 't' test; n=4) at all voltages recorded. However the currents were suppressed by 10 μM linopirdine, a direct KCNQ channel inhibitor. In panels B and C, filled circles indicate control KCNQ5 currents, open circles indicate KCNQ5 currents in the presence of OAG, filled triangles indicate KCNQ5 current in the presence of 10 μM linopirdine. D. Representative time course of 100 μM OAG-induced Ca^{2+} spiking in control and TRPC6shRNA-expressing A7r5 cells, and control cells pre-

incubated with a selective PKC inhibitor Ro-31-8220 (2 μM). Pre-incubation with Ro-31-8220 completely abolished OAG-induced Ca^{2+} spiking. E. Bar graph shows the latency to onset of OAG-induced Ca^{2+} spiking in TRPC6shRNA expressing cells and control A7r5 cells. *Significantly greater than control ($p<0.05$, Student's paired 't' test; n=4 for each condition). F. Bar graph shows the frequency of Ca^{2+} spiking with OAG treatment in TRPC6shRNA expressing cells and control A7r5 cells. No significant difference from control ($p>0.1$, Student's paired 't' test; n=4, for each condition).

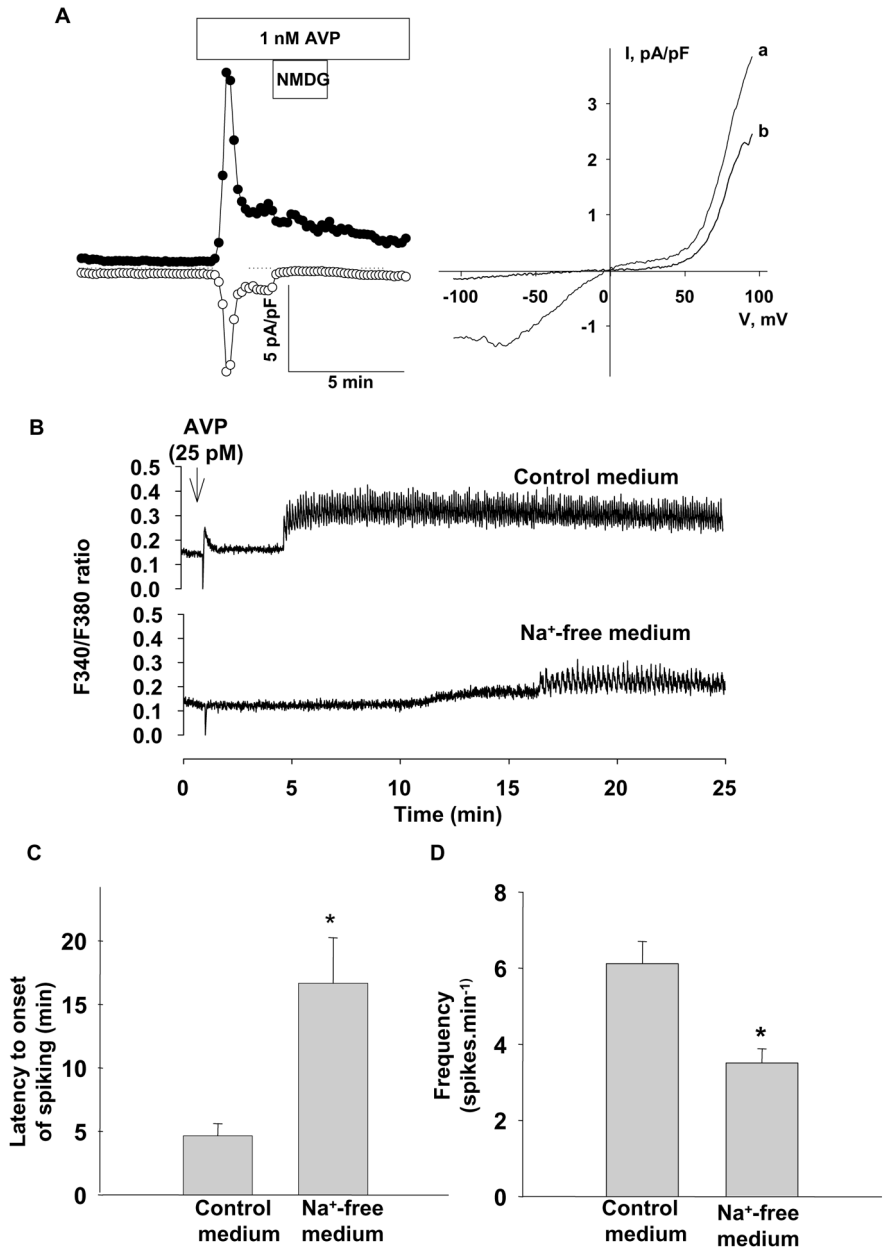

Figure 7. Na^+-free medium eliminates inward I_{CAT} and reduces frequency/increases latency to AVP-stimulated Ca^{2+} spiking

A. Representative time course (left) and IV curve (right) shows reduction in I_{CAT} activated by 1 nM AVP, when Na^+ in the external solution was replaced with NMDG, an impermeant cation. Outward currents were measured at +85 mV (filled circles) and inward currents were measured at −115 mV (open circles). Inward currents were abolished when Na^+ was replaced with NMDG (representative of 3 similar experiments). IV graphs show I_{CAT} recordings before replacement with NMDG (a) and after replacement with NMDG (b). B. Representative time course of 25 pM AVP-induced Ca^{2+} spiking in A7r5 cells in control medium and Na^+-free medium. C. Bar graph shows the latency to onset of Ca^{2+} spiking in A7r5 cells in Na^+-free medium and control medium. *Significantly greater than control ($p<0.05$, Student's paired 't' test; n=4 for each condition). D. Bar graph shows the frequency of Ca^{2+} spiking in A7r5 cells

in control medium and Na^+-free medium. *Significantly lower than control ($p<0.01$, Student's paired 't' test; n=4 for each condition).

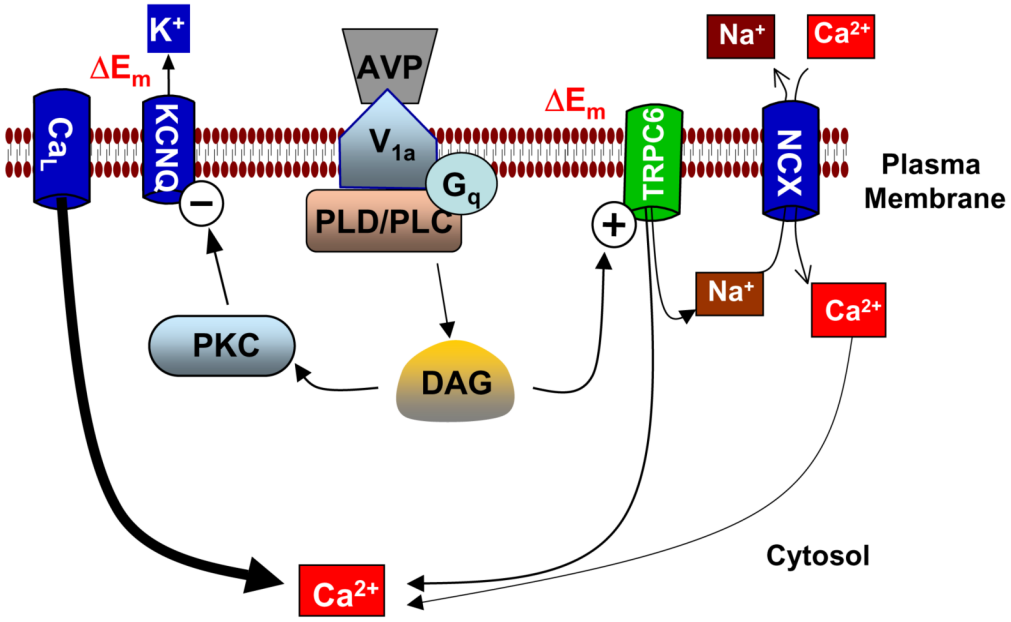

Figure 8. Hypothetical signal transduction pathway for AVP-stimulated Ca^{2+} spiking in vascular smooth muscle cells

AVP activates V_{1a} G_q-coupled receptors resulting in downstream production of diacylglycerol (DAG) by phospholipases D and C (PLD and PLC). DAG in turn activates protein kinase C (PKC) and also directly activates TRPC6 non-selective cation channels. DAG-induced PKC activation causes suppression of K^+ efflux via KCNQ5 channels. PKC-mediated suppression of KCNQ5 currents, combined with direct activation of TRPC6 channels by DAG, causes membrane depolarization and Ca^{2+} influx through voltage-sensitive Ca^{2+} channels. Influx of Na^+ and Ca^{2+} through TRPC6 channels contribute modestly to the increase in $[Ca^{2+}]_i$ by membrane depolarization and reversal of Na^+/Ca^{2+}-exchanger.